

Real and complex behavior for networks of coupled logistic maps

Anca R#dulescu & Ariel Pignatelli

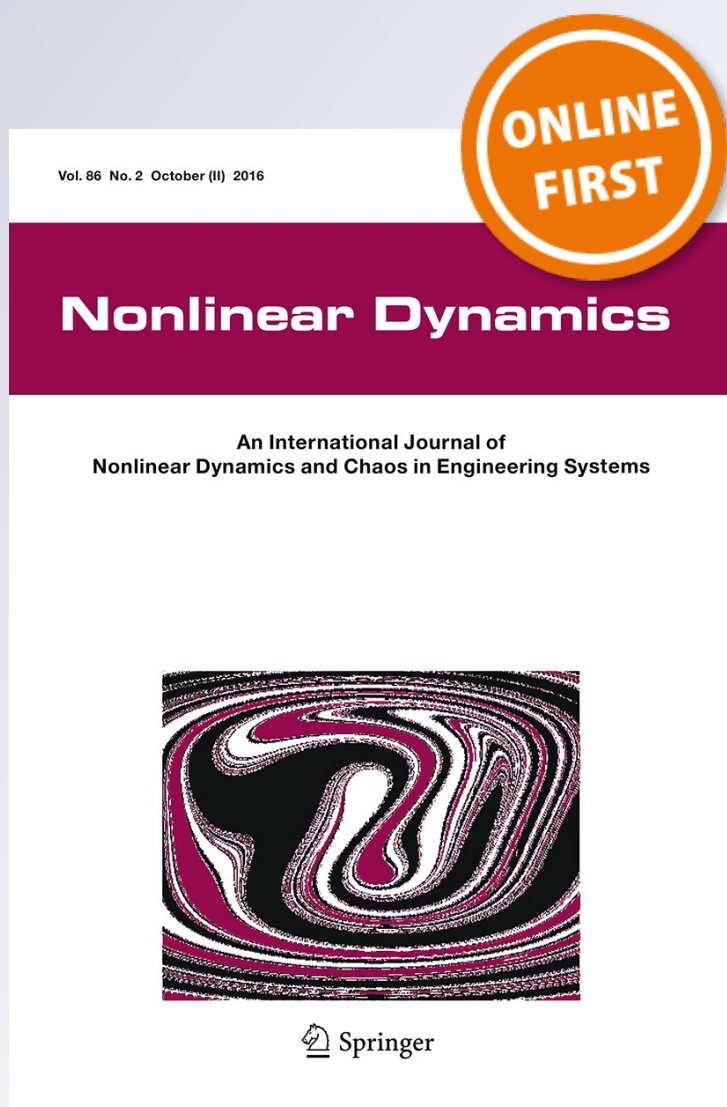
Nonlinear Dynamics

An International Journal of Nonlinear
Dynamics and Chaos in Engineering
Systems

ISSN 0924-090X

Nonlinear Dyn

DOI 10.1007/s11071-016-3115-4



Your article is protected by copyright and all rights are held exclusively by Springer Science +Business Media Dordrecht. This e-offprint is for personal use only and shall not be self-archived in electronic repositories. If you wish to self-archive your article, please use the accepted manuscript version for posting on your own website. You may further deposit the accepted manuscript version in any repository, provided it is only made publicly available 12 months after official publication or later and provided acknowledgement is given to the original source of publication and a link is inserted to the published article on Springer's website. The link must be accompanied by the following text: "The final publication is available at link.springer.com".

Real and complex behavior for networks of coupled logistic maps

Anca Rădulescu · Ariel Pignatelli

Received: 7 May 2016 / Accepted: 24 September 2016
© Springer Science+Business Media Dordrecht 2016

Abstract Many natural systems are organized as networks, in which the nodes interact in a time-dependent fashion. The object of our study is to relate connectivity to the temporal behavior of a network in which the nodes are (real or complex) logistic maps, coupled according to a connectivity scheme that obeys certain constraints, but also incorporates random aspects. We investigate in particular the relationship between the system architecture and possible dynamics. In the current paper, we focus on establishing the framework, terminology and pertinent questions for low-dimensional networks. A subsequent paper will further address the relationship between hardwiring and dynamics in high-dimensional networks. For networks of both complex and real node maps, we define extensions of the Julia and Mandelbrot sets traditionally defined in the context of single-map iterations. For three different model networks, we use a combination of analytical and numerical tools to illustrate how the system behavior (measured via topological properties of the *Julia set*) changes when perturbing the underlying adjacency graph. We differentiate between the effects on dynamics of different perturbations that directly modulate network connectivity: increasing/decreasing edge

weights, and altering edge configuration by adding, deleting or moving edges. We discuss the implications of extending Fatou–Julia theory from iterations of single maps, to iterations of ensembles of maps coupled as nodes in a network.

Keywords Coupled complex maps · Nonlinear network architecture · Uni-Julia set · Equi-Mandelbrot set · Multi-orbit · Connectivity

1 Introduction

1.1 Network architecture as a system parameter

Because many natural systems are organized as networks, in which the nodes (be they cells, individuals, populations or Web servers) interact in a time-dependent fashion, the study of networks has been an important focus in recent research. One of the particular points of interest has been the question of how the hardwired *structure* of a network (its underlying graph) affects its *function*, for example in the context of optimal information storage or transmission between nodes along time. It has been hypothesized that there are two key conditions for optimal function in such networks: a well-balanced adjacency matrix (the underlying graph should appropriately combine robust features and random edges) and well-balanced connection strengths, driving optimal dynamics in the system. However, only recently has mathematics started to study rigorously

A. Rădulescu (✉)
Department of Mathematics, State University of New York
at New Paltz, New Paltz, NY 12561, USA
e-mail: radulesa@newpaltz.edu

A. Pignatelli
Department of Mechanical Engineering, State University of New
York at New Paltz, New Paltz, NY 12561, USA

(through a combined graph theoretical and dynamic approach) the effects of configuration patterns on the efficiency of network function, by applying graph theoretical measures of segregation (clustering coefficient, motifs, modularity, rich clubs), integration (path length, efficiency) and influence (node degree, centrality). Various studies have been investigating the sensitivity of a system's temporal behavior to removing/adding nodes or edges at different places in the network structure and have tried to relate these patterns to applications to natural networks.

Brain functioning is one of the most intensely studied contexts which requires our understanding of the tight inter-connections between system architecture and dynamics. The brain is organized as a “dynamic network,” self-interacting in a time-dependent fashion at multiple spatial and temporal scales, to deliver an optimal range for biological functioning. The way in which these modules are wired together in large networks that control complex cognition and behavior is one of the great scientific challenges of the twenty-first century, currently being addressed by large-scale research collaborations, such as the Human Connectome Project. Graph theoretical studies of empirical data support certain generic topological properties of brain architecture, such as modularity, small worldness, the existence of hubs and “rich clubs” [4, 19, 20].

In order to explain how connectivity patterns may affect the system's dynamics (e.g., in the context of stability and synchronization in networks of coupled neural populations), and thus the observed behavior, a lot of effort has been thus invested toward formal modeling approaches, using a combination of analytical and numerical methods from nonlinear dynamics and graph theory, in both biophysical models [8] and simplified systems [18]. These analyses revealed a rich range of potential dynamic regimes and transitions [3], shown to depend as much on the coupling parameters of the network as on the arrangement of the excitatory and inhibitory connections [8]. The construction of a realistic, data-compatible computational model has been subsequently found to present many difficulties that transcend the existing methods from nonlinear dynamics and may in fact require: (1) new analysis and book-keeping methods and (2) a new framework that would naturally encompass the rich phenomena intrinsic to these systems—both of which aspects are central to our proposed work.

In a paper by Rădulescu and Verduzco-Flores [16], one of the authors of this paper first explored the idea of having network connectivity as a bifurcation parameter for ensemble dynamics in a network of coupled oscillators and investigated the relationship between classes of system architectures and classes of their possible dynamics. As expected, when translating connectivity patterns to network dynamics, the main difficulties were raised by the combination of graph complexity and the system's intractable dynamic richness. In order to break down and better understand this dependence, we started to investigate it in simpler theoretical models, where one may more easily identify and pair specific structural patterns to their effects on dynamics. The logistic family is historically perhaps the most-studied family of maps in nonlinear dynamics, whose behavior is by now relatively well understood. Therefore, we started by looking in particular at how dynamic behavior depends on connectivity in simple networks with logistic nodes. This paper focuses on definitions, concepts and observations in low-dimensional networks. Future work will address larger networks, as well as other classes of maps.

Dynamic networks with discrete nodes and the dependence of their behavior on connectivity parameters have been previously described in several contexts over the past two decades. For example, in an early paper, Wang considered a simple neural network of only two excitatory/inhibitory neurons and analyzed it as a parameterized family of two-dimensional maps, proving existence of period doubling to chaos and strange attractors in the network [21]. Masolle and Attay [14] have found that in networks of delay-coupled logistic maps, synchronization regimes and formation of anti-phase clusters depend on coupling strength and on the edge topology (characterized by the spectrum of the graph Laplacian) [1]. Yu et al. [22] have constructed and studied a network, wherein the undirected edges symbolize the nodes' relation of adjacency in an integer sequence obtained from the logistic mapping and the top integral function.

In our present work, we focus on investigating, in the context of networked maps, extensions of the Julia and Mandelbrot sets traditionally defined for single-map iterations. For three different model networks, we use a combination of analytical and numerical tools to illustrate how the system behavior (measured via topological properties of the *Julia sets*) changes when perturbing the underlying adjacency graph. We differ-

entiate between the effects on dynamics of different perturbations that directly modulate network connectivity: increasing/decreasing edge weights, and altering edge configuration by adding, deleting or moving edges. We discuss the implications of considering a rigorous extension of Fatou–Julia theory known to apply for iterations of single maps, to iterations of ensembles of maps coupled as nodes in a network.

1.2 Networking logistic maps

The logistic map is historically perhaps the best-known family of maps in nonlinear dynamics. Iterations of one single quadratic function have been studied starting in the early nineteenth century, with the work of Fatou and Julia.

The prisoner set of a map f is defined as the set of all points in the complex dynamic plane, whose orbits are bounded. The escape set of a complex map is the set of all points whose orbits are unbounded. The Julia set of f is defined as their common boundary $J(f)$. The filled Julia set is the union of prisoner points with their boundary $J(f)$.

For polynomial maps, it has been shown that the connectivity of a map's Julia set is tightly related to the structure of its critical orbits (i.e., the orbits of the map's critical points). Due to extensive work spanning almost one century, from Julia [10] and Fatou [7] until recent developments [2, 15], we now have the following:

Fatou–Julia Theorem. *For a polynomial with at least one critical orbit unbounded, the Julia set is totally disconnected if and only if all the bounded critical orbits are aperiodic.*

For a single iterated logistic map [5, 6], the Fatou–Julia Theorem implies that the Julia set is either totally connected, when the orbit of the critical point 0 is bounded, or totally disconnected, when the orbit of the critical point 0 is unbounded. In previous work, the authors showed that this dichotomy breaks in the case of random iterations of two maps [17]. In our current work, we focus on extensions for networked logistic maps. Although Julia and Mandelbrot sets have been studied somewhat in connection with coupled systems [9], none of the existing work seems to address the basic problems of how these sets can be defined for networks of maps, how different aspects of the network hardware affect the topology of these sets, and whether there is any Fatou–Julia-type result in this context.

These are some of the questions addressed in this paper, which is organized as follows: In Sect. 2, we introduce definitions of our network setup, as well as of the extensions of Mandelbrot and Julia sets that we will be studying. In order to illustrate some basic ideas and concepts, we concentrate on three examples of 3-dimensional networks, which differ from each other in edge distribution, and whose connectivity strengths are allowed to vary. In Sect. 3, we focus on the behavior of these 3-dimensional models when we consider the nodes as complex iterated variables. We analyze the similarities and differences between node-wise behavior in each case, and we investigate the topological perturbations in one-dimensional complex slices of the Mandelbrot and Julia sets, as the connectivity changes from one model to the next, through intermediate stages. In Sect. 4, we address the same questions for real logistic nodes, with the advantage of being able to visualize the network Mandelbrot and Julia sets, as 3-dimensional real objects. In both sections, we conjecture weaker versions of the Fatou–Julia theorem, relating points in the Mandelbrot set with connectivity properties of the corresponding Julia sets. Finally, in Sect. 5, we interpret our results both mathematically and in the larger context of network sciences. We also briefly preview future work on high-dimensional networks and on networks with adaptable nodes and edges.

2 Our models of networked logistic maps

We consider a set of n nodes coupled according to the edges of an oriented graph, with adjacency matrix $A = (A_{jk})_{j,k=1}^n$ (on which one may impose additional structural conditions, related to edge density or distribution). In isolation, each node x_k , $1 \leq k \leq n$, functions as a discrete nonlinear map f_k , changing at each iteration $t \in \mathbb{N}$ as $x_k(t) \rightarrow x_k(t+1)$. When coupled as a network with adjacency A , each node will also receive contributions through the incoming edges from the adjacent nodes. Throughout this paper, we will consider an additive rule of combining these contributions, for a couple of reasons: first, summing weighted incoming inputs is one simple, yet mathematically non-trivial way to introduce the cross talk between nodes; second, summing weighted inputs inside a nonlinear integrating function is reminiscent of certain mechanisms studied in the natural sciences (such as the integrate and fire neural mechanism studied in our previous work in the

context of coupled dynamics). The coupled system will then have the following general form:

$$x_k(t) \longrightarrow x_k(t + 1) = f_k \left(\sum_{j=1}^n g_{jk} A_{jk} x_j \right)$$

where g_{jk} are the weights along the adjacency edges. One may view this system simply as an iteration of an n -dimensional map $f = (f_k)_{k=1}^n$, with $f: \mathbb{R}^n \rightarrow \mathbb{R}^n$ (in the case of real-valued nodes), or, respectively, $f: \mathbb{C}^n \rightarrow \mathbb{C}^n$ (in the case of complex-valued nodes). The new and exciting aspect that we are proposing in our work is to study the dependence of the coupled dynamics on the parameters, in particular on the coupling scheme (adjacency matrix)—viewed itself as a system parameter. To fix these ideas, we focused first on defining these questions and proposing hypotheses for the case of quadratic node dynamics. The logistic family is one of the most-studied families of maps in the context of both real and complex dynamics of a single variable. It was also the subject of our previous modeling work on random iterations.

In this paper in particular, we will work with quadratic node maps, with their traditional parametrization $f_c(z) = z^2 + c$, with $f_c: \mathbb{C} \rightarrow \mathbb{C}$ and $c \in \mathbb{C}$ for the complex case and $f_c: \mathbb{R} \rightarrow \mathbb{R}$ and $c \in \mathbb{R}$ for the real case. The network variable will be called, respectively, $(z_1, \dots, z_k) \in \mathbb{C}^n$ in the case of complex nodes, and $(x_1, \dots, x_k) \in \mathbb{R}^n$ in the case of real nodes. We consider both the particular case of identical quadratic maps (equal c values) and the general case of different maps attached to the nodes throughout the network. In both cases, we aim to study the asymptotic behavior of iterated node-wise orbits, as well as of the n -dimensional orbits (which we will call multi-orbits). As in the classical theory of Fatou and Julia, we will investigate when orbits escape to infinity or remain bounded, and how much of this information is encoded in the critical multi-orbit of the system.

For the following definitions, fix the network (i.e., fix the adjacency A and the edge weights g). To avoid redundancy, we give definitions for the complex case, but they can be formulated similarly for real maps:

Definition 2.1 For a fixed parameter $(c_1, \dots, c_n) \in \mathbb{C}^n$, we call the **filled multi-Julia set** of the network the locus of $(z_1, \dots, z_n) \in \mathbb{C}^n$ which produces a bounded multi-orbit in \mathbb{C}^n . We call the **filled uni-Julia set** the locus of $z \in \mathbb{C}$ so that $(z, \dots, z) \in \mathbb{C}^n$ produces a bounded multi-orbit. The **multi-Julia set (or the**

multi-J set) of the network is defined as the boundary in \mathbb{C}^n of the filled multi-Julia set. Similarly, one defines the **uni-Julia set (or uni-J set)** of the network as the boundary in \mathbb{C} of its filled counterparts.

Definition 2.2 We define the **multi-Mandelbrot set (or the multi-M set)** of the network the parameter locus of $(c_1, \dots, c_n) \in \mathbb{C}^n$ for which the multi-orbit of the critical point $(0, \dots, 0)$ is bounded in \mathbb{C}^n . We call the **equi-Mandelbrot set (or the equi-M set)** of the network the locus of $c \in \mathbb{C}$ for which the critical multi-orbit is bounded for the **equi-parameter** $(c_1, c_2, \dots, c_n) = (c, c, \dots, c) \in \mathbb{C}^n$. We call the **k th node equi-M set** the locus $c \in \mathbb{C}$ such that the component of the multi-orbit of $(0, \dots, 0)$ corresponding to the k th node remains bounded in \mathbb{C} .

We study, using a combination of analytical and numerical methods, how the structure of the Julia and Mandelbrot sets varies under perturbations of the node-wise dynamics (i.e., under changes of the quadratic multi-parameter (c_1, c_2, \dots, c_n)) and under perturbations of the coupling scheme (i.e., of the adjacency matrix A and of the coupling weights g). In this paper, we start with investigating these questions in small (3-dimensional) networks, with specific adjacency configurations. In a subsequent paper, we will move to investigate how similar phenomena may be quantified and studied analytically and numerically in high-dimensional networks. In both cases, we are interested in particular in observing differences in the effects on dynamics of three different aspects of the network architecture: (1) increasing/decreasing edge weights, (2) increasing/decreasing edge density and (3) altering edge configuration by adding, deleting or moving edges.

While a desired objective would be to obtain general results for all network sizes (since many natural networks are large), we start by studying simple, low-dimensional systems. In this study, we focus on simple networks formed of three nodes, connected by different network geometries and edge weights. To fix our ideas, we will follow and illustrate three structures in particular (also see Fig. 1): (1) Two input nodes z_1 and z_2 are self-driven by quadratic maps, and the single output node z_3 is driven symmetrically by the two input nodes; z_1 additionally communicates with z_2 via an edge of variable weight a , which can take both positive and negative values. We will call this the **simple dual model**. (2) In addition to the simple dual scheme, the output node z_3 is also self-driven, i.e., there is a

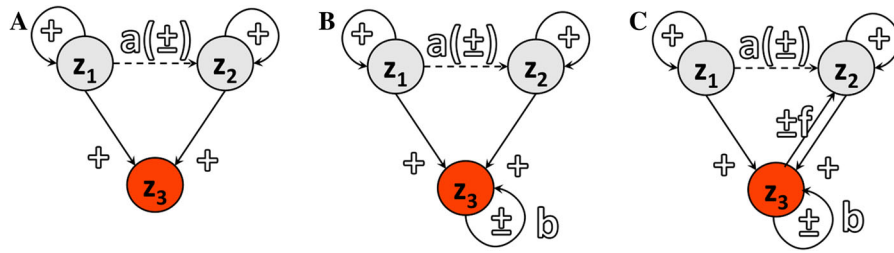


Fig. 1 Three-dimensional networks used as simple coupling setups to study the dependence of the Mandelbrot set topology on coupling strength and on network architecture. We will call

these three constructions: **a** the simple dual model, **b** the self-drive model and **c** the feedback model

self-loop on z_3 of weight b (which can be positive or negative). We will call this the *self-drive model*. (3) In addition to the self-drive model, there is also feedback from the output node z_3 into the node z_2 , via a new edge of variable weight f . We will call this the *feedback model*. Unless specified, edges have positive unit weight. Notice that the same effect as negative feed-forward edges from z_1 and z_2 into z_3 can be obtained by changing the sign of b , etc. The three connectivity models we chose to study and compare are described by the equations below:

Simple dual model	Self-drive model	Feedback model
$z_1 \rightarrow z_1^2 + c_1$	$z_1 \rightarrow z_1^2 + c_1$	$z_1 \rightarrow z_1^2 + c_1$
$z_2 \rightarrow (az_1 + z_2)^2 + c_2$	$z_2 \rightarrow (az_1 + z_2)^2 + c_2$	$z_2 \rightarrow (az_1 + z_2 + fz_3)^2 + c_2$
$z_3 \rightarrow (z_1 + z_2)^2 + c_3$	$z_3 \rightarrow (z_1 + z_2 + bz_3)^2 + c_3$	$z_3 \rightarrow (z_1 + z_2 + bz_3)^2 + c_3$

For a fixed multi-parameter $(c_1, c_2, c_3) \in \mathbb{C}^3$ for example, one can see all three systems as generated by a network map $f = (f_{c_1}, f_{c_2}, f_{c_3}) : \mathbb{C}^3 \rightarrow \mathbb{C}^3$, defined as $f(z_1, z_2, z_3) = (f_{c_1}([Az]_1), f_{c_2}([Az]_2), f_{c_3}([Az]_3))$, for any $z = (z_1, z_2, z_3)^t \in \mathbb{C}^3$.

We try to classify and understand the effects that coupling changes have on the topology of multi- J and multi- M sets for both complex and real networked maps. We do not expect all classical topology results on the Julia and Mandelbrot sets for single maps (e.g., Fatou–Julia theorem, or connectivity of the Mandelbrot set) to carry out for networks of coupled maps. However, since the topology of the full sets in \mathbb{C}^3 is somewhat harder to inspect, we study as a first step their equi-slices and node-wise equi-slices, which are objects in \mathbb{C} .

We will track and compare in particular the differences between the three models, but also the geometric and topological changes produced on the equi-

slices within each one model for different values of the parameters a, b and f . None of these results, however, can be directly extrapolated to similar conclusions on the full sets. To offer some insight into the latter, we study the multi- M and multi- J sets in the context of real maps, for which the objects can be visualized in \mathbb{R}^3 .

3 Complex coupled maps

3.1 Equi-Mandelbrot sets

A first intuitive question is when the nodes of the network have similar behavior, and whether if one node-wise orbit is bounded, the others will remain bounded. This relationship is trivial to establish in some cases, such as, for example, in the simple dual model with independent input nodes (i.e., $a = 0$). Indeed, in this model, for any fixed $c \in \mathbb{C}$, the origin's orbit in \mathbb{C}^3 under (f_c, f_c, f_c) can be described as:

$$\begin{aligned} z_1 : 0 &\rightarrow c \rightarrow c^2 + c \rightarrow (c^2 + c)^2 + c \rightarrow \dots \\ z_2 : 0 &\rightarrow c \rightarrow c^2 + c \rightarrow (c^2 + c)^2 + c \rightarrow \dots \\ z_3 : 0 &\rightarrow c \rightarrow (2c)^2 + c \rightarrow 4(c^2 + c)^2 + c \dots \end{aligned}$$

The projection of the orbit in any of the three components only depends on the previous states of z_1 and z_2 , and these three sequences are simultaneously bounded in \mathbb{C} ; hence, the node-specific equi-Mandelbrot sets are all identical with the traditional Mandelbrot set. Some basic connections between node-wise equi- M sets in each of the three models are stated below. We will prove these incrementally (recall that the dual model is a particular case of self-drive for $b = 0$, and the self-drive is a particular case of feedback model with $f = 0$).

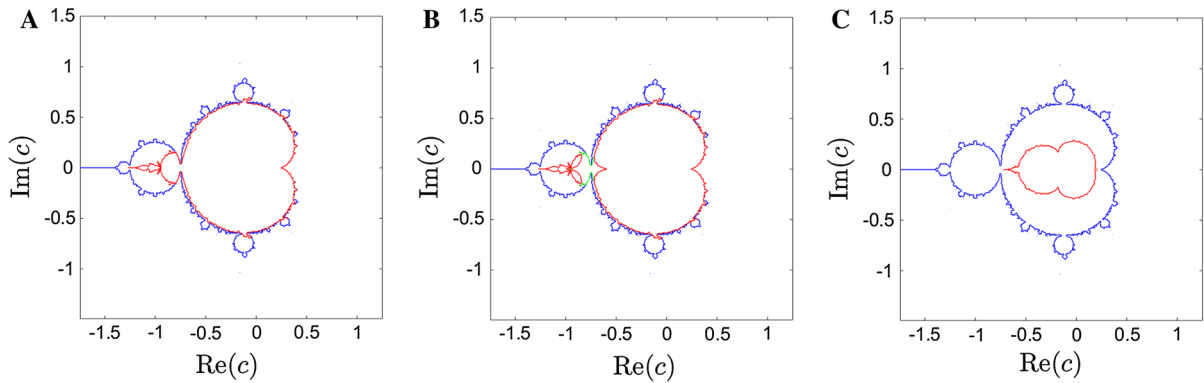


Fig. 2 Differences between node-specific equi-Mandelbrot slices, for different connectivity patterns. **a** For the simple dual model with $a = -2/3$, the equi-Mandelbrot set for the nodes z_2 and z_3 are identical (red), but different from the set for the node z_1 (blue). **b** For the self-drive model with negative feedback, $a = -2/3$ and $b = 1/3$, the equi-Mandelbrot sets for the three nodes z_1 , z_2 and z_3 (shown, respectively, in blue, green and red)

are all different. **c** For the feedback model with negative feedback, $a = -2/3$ and $b = 1/3$, $f = -1$, the equi-Mandelbrot set for the nodes z_2 and z_3 are identical (red), but different from the set for the node z_1 (blue). In all panels, the computations were generated based on $L = 100$ iterations, and for an escape radius of $R = 10$. (Color figure online)

Proposition 3.1 *In the simple dual model, the node-wise equi- M sets for the nodes z_2 and z_3 are identical subsets of the traditional Mandelbrot set (which is the equi- M set for node z_1).*

Proof The simple case $a = 0$ was already discussed. We will now assume $a \neq 0$. Suppose the critical orbit for node z_2 is bounded by a radius M , that is $z_2(n) \leq M$, for all n . Hence (omitting the subscript n for simplicity):

$$\begin{aligned} M &\geq |z_2(n+1)| = |(az_1 + z_2)^2 + c| \\ &\geq |az_1 + z_2|^2 - |c| \implies \sqrt{M + |c|} \\ &\geq |az_1 + z_2| \geq |az_1| - |z_2| \end{aligned}$$

It follows that:

$$\begin{aligned} |az_1| &\leq \sqrt{M + |c|} + |z_2| \\ &\leq \sqrt{M + |c|} + M, \text{ where } a \neq 0 \end{aligned} \tag{1}$$

Hence, if the orbit z_2 is bounded, then the orbit of z_1 is bounded. This applies in particular for the critical orbit, showing that the equi- M set for z_2 is a subset of the equi- M set for z_1 .

We will next show that, for the simple dual model, corresponding orbits of z_2 and z_3 are simultaneously bounded. For instance, suppose that an orbit $z_2(n)$ is bounded by $M > 0$. It follows, as shown above, that the corresponding $z_1(n)$ orbit is bounded by some $K > 0$.

Then:

$$\begin{aligned} z_3(n+1) &= |(z_1 + z_2)^2 + c| \leq |z_1 + z_2|^2 + |c| \\ &= |(az_1 + z_2) + (1-a)z_1|^2 + |c| \\ &\leq (|az_1 + z_2| + |1-a||z_1|)^2 \\ &\quad + |c| \leq (M + |1-a|K)^2 + |c| \end{aligned} \tag{2}$$

Hence, the orbit $z_3(n)$ is bounded. The converse is similar, showing that the z_2 and z_3 equi- M sets are always identical subsets of the z_1 equi- M set in the simple dual model. In Fig. 2a, we show that these are generally strict subsets and that a non-symmetric communication $a \neq 0$ can introduce significant differences between the traditional Mandelbrot set of the independent node z_1 and the equi- M subsets for z_2 and z_3 . For example, it is not hard to show that, for $a = -2/3$ (illustrated in Fig. 2a), the point $c = -2$ belongs to the Mandelbrot set of z_1 (the critical orbit has period three), but not to the equi- M set of z_2 and z_3 . \square

An additional self-drive $b \neq 0$ applied to the output node changes the balance of inputs to z_3 , in the following sense:

Proposition 3.2 *In the self-drive model, the node-wise equi- M sets of z_2 and z_3 remain subsets of the standard Mandelbrot set, but the equi- M set of z_3 is strictly contained in the equi- M set of z_2 (Fig. 2b).*

Proof To prove the first part of this statement, take a point c in the equi- M set of z_3 , meaning that the orbit of z_3 is bounded: There exists $M > 0$ such that $|z_3(n)| \leq M$, for all $n \geq 0$. We can express:

$$\begin{aligned} |z_3(n+1)| &= |(z_1 + z_2 + bz_3)^2 + c| \\ &\geq |z_1 + z_2 + bz_3|^2 - |c| \end{aligned}$$

It follows that:

$$\begin{aligned} |z_1 + z_2| - |bz_3| &\leq |z_1 + z_2 + bz_3| \\ &\leq \sqrt{|z_3(n+1)| + |c|} \leq \sqrt{M + |c|} \end{aligned}$$

Hence,

$$\begin{aligned} |z_1 + z_2| &\leq \sqrt{M + |c|} + |bz_3| \\ &\leq \sqrt{M + |c|} + |b|M \end{aligned} \tag{3}$$

that is, the sequence $\xi(n) = z_1(n) + z_2(n)$ is also bounded in radius by $K_1 = \sqrt{M + |c|} + |b|M$. Let us recall that

$$\begin{aligned} |\xi(n+1)| &= |z_1^2 + c + (az_1 + z_2)^2 + c| \\ &= |z_1^2 + [(a-1)z_1 + \xi]^2 + 2c| \\ &= z_1^2 + (a-1)^2 z_1^2 + 2(a-1)z_1\xi + \xi^2 + 2c \\ &= \left| \left[\sqrt{(a-1)^2 + 1}z_1 + \frac{(a-1)\xi}{\sqrt{(a-1)^2 + 1}} \right]^2 \right. \\ &\quad \left. + \xi^2 \left(1 - \frac{(a-1)^2}{(a-1)^2 + 1} \right) + 2c \right| \\ &\geq \left| \sqrt{(a-1)^2 + 1}z_1 + \frac{(a-1)\xi}{\sqrt{(a-1)^2 + 1}} \right|^2 \\ &\quad - \left| \frac{\xi^2}{(a-1)^2 + 1} + 2c \right| \end{aligned} \tag{4}$$

It follows that

$$\begin{aligned} |k_1 z_1 + k_2 \xi|^2 &\leq |\xi(n+1)| + \left| \frac{\xi^2}{(a-1)^2 + 1} + 2c \right| \\ \implies |k_1 z_1 + k_2 \xi| &\leq K_2 \end{aligned} \tag{5}$$

where $k_1 = \sqrt{(a-1)^2 + 1}$, $k_2 = \frac{(a-1)}{\sqrt{(a-1)^2 + 1}}$

and $K_2 = \sqrt{K_1 + \frac{K_1^2}{(a-1)^2 + 1} + |2c|}$. It follows that $|k_1 z_1| \leq K_2 + |k_2 \xi| \leq K_2 + |k_2|K_1$; hence, the orbit of the node z_1 is also bounded. Now recall that: $\xi = z_1 + z_2$ is bounded. Since we can write $|z_2| = |\xi - z_1| \leq |\xi| + |z_1|$, it follows that z_2 is also

bounded. This proves that the equi- M set of z_3 is a subset of the equi- M set of z_2 , which is in turn a subset of the traditional Mandelbrot set (i.e., the equi- M set of z_1).

To prove that these inclusions are strict, one can easily find points which are in the equi- M set of z_2 , but not in the equi- M set of z_3 . For example, for the parameters in Fig. 2b, $c = -3/4$ is in the M set of z_1 (the critical orbit is eventually fixed), and it is in the equi- M set of z_2 , but it is not in the M set of z_3 . Indeed, for this particular c value, $z_1(n) = -3/4$, for all $n \geq 2$ (fixed point). Since $a = -2/3$, we can calculate, for $n \geq 2$: $z_2(n+1) = [1/2 + z_2(n)]^2 - 3/4 = z_2^2(n) + z_2(n) - 1/2$, with $z_2(2) = -3/4$. One can easily show that if $z_2 \in [-1, 0]$, then $z_2^2 + z_2 - 1/2 \in [-1, 0]$; hence, it follows by induction that the critical orbit of z_2 is contained in $[-1, 0]$ (i.e., bounded). \square

Finally, introducing any arbitrary feedback $f \neq 0$ recouples the behavior of nodes z_2 and z_3 , producing a common equi-Mandelbrot set, largely shrunk from the simple dual version:

Proposition 3.3 *In the feedback model with $b \neq 0$ and $f \neq 0$, the node-wise equi- M sets for the nodes z_2 and z_3 are again identical subsets of the traditional Mandelbrot set (Fig. 2c).*

Proof The proof is a slightly more general version of that for Proposition 3.2. Suppose first that the orbit of z_3 is bounded in radius by M . As before, it follows that:

$$\begin{aligned} M &\geq |z_3(n+1)| = |(z_1 + z_2 + bz_3)^2 + c| \\ &\geq |z_1 + z_2 + bz_3|^2 - |c| \end{aligned}$$

Hence, as before

$$|\xi| = |z_1 + z_2| \leq |b|M + \sqrt{M + |c|} = K_1$$

Call $\psi = \xi + fz_3$ so that:

$$|\psi| \leq |\xi| + |fz_3| \leq K_1 + |f|M = K_2$$

We calculate:

$$\begin{aligned} |\xi(n+1)| &= |z_1^2 + (az_1 + z_2 + fz_3)^2 + 2c| \\ &= |z_1^2 + [(a-1)z_1 + \xi + fz_3]^2 + 2c| \\ &= |z_1^2 + [(a-1)z_1 + \psi]^2 + 2c| \\ &= |z_1^2 + (a-1)^2 z_1^2 + 2(a-1)z_1\psi + \psi^2 + 2c| \\ &= \left| \left([1 + (a-1)^2]z_1^2 + 2(a-1)z_1\psi \right. \right. \end{aligned}$$

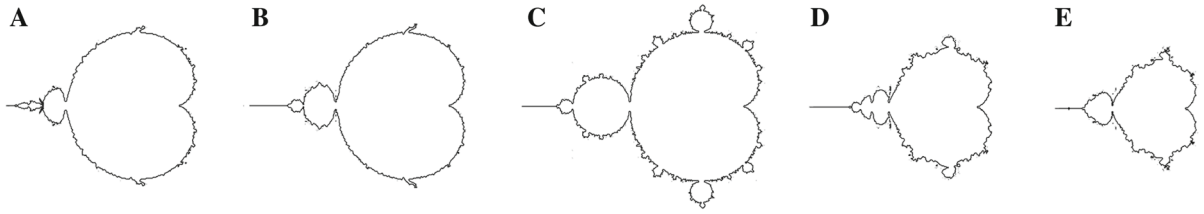


Fig. 3 Differences between equi-Mandelbrot slices in the case of the simple dual model, as the cross talk parameter a increases: **a** $a = -2/3$, **b** $a = -1/3$, **c** $a = 0$ (traditional Mandelbrot set), **d** $a = 1/3$ and **e** $a = 2/3$

$$\begin{aligned}
 & + \frac{a-1}{(a-1)^2+1} \psi^2 \Big) \\
 & + \left(1 - \frac{a-1}{(a-1)^2+1} \right) \psi^2 + 2c \Big| \\
 & = \left| (k_1 z_1 + k_2 \psi)^2 + k_3 \psi^2 + 2c \right| \quad (6)
 \end{aligned}$$

where $k_1 = \sqrt{(a-1)^2+1}$, $k_2 = \frac{a-1}{(a-1)^2+1}$ and $k_3 = \frac{1}{(a-1)^2+1}$. Hence

$$\begin{aligned}
 |k_1 z_1 + k_2 \psi| & \leq |\xi(n+1)| + k_3 |\psi|^2 + 2|c| \\
 & \leq K_1 + k_3 K_2^2 + 2|c| = K_3 \quad (7)
 \end{aligned}$$

Since ψ is bounded, it follows that z_1 is bounded. Since ξ is bounded, it follows that z_2 is bounded. This proves that the equi- M set of z_3 is a subset of the equi- M sets of z_2 and z_1 .

Conversely, suppose that the orbit of z_2 is bounded in radius by $M > 0$. It follows that the sequence corresponding to $az_1 + fz_3$ is also bounded. Recall that the case $f = 0$ was covered by the previous proposition; hence, we can assume now that $f \neq 0$. Hence, $\xi = hz_1 + bz_3$ is bounded by a constant K_1 , where $h = ba/f$, for $f \neq 0$. As before, call $\psi = hz_1 + bz_3 + z_2$, and notice that ψ is bounded by $K_1 + M$.

$$\begin{aligned}
 |\xi(n+1)| & = |h(z_1^2 + c) + b[(z_1 + z_2 + bz_3)^2 + c]| \\
 & = |hz_1^2 + b[\psi + (1-h)z_1]^2 + c(h+b)| \\
 & = |hz_1^2 + b(1-h)^2 z_1^2 + 2b(1-h)z_1 \psi \\
 & \quad + b\psi^2 + c(h+b)| \quad (8)
 \end{aligned}$$

If $k_1^2 = h + b(1-h)^2 \neq 0$, then we again have:

$$|\xi(n+1)| = |(k_1 z_1 + k_2 \psi)^2 + k_3 \psi^2 + c(h+b)| \quad (9)$$

where $k_2 = \frac{b(1-h)}{k_1}$ and $k_3 = b - k_2^2$. Since ψ is bounded, it follows that z_1 is bounded. Since ξ is bounded, it further follows that z_3 is bounded.

We look separately at the case $k_1^2 = h + b(1-h)^2 = 0$, for which Eq. (8) becomes:

$$|\xi(n+1)| = |2b(1-h)z_1 \psi + b\psi^2 + c(h+b)| \quad (10)$$

Since $b \neq 0$, it follows that $b(1-h) \neq 0$. Since ξ and ψ are bounded, it immediately follows that z_1 is also bounded.

This concludes the proof that the equi- M sets of z_2 and z_3 are identical, and both subsets of the equi- M set of z_1 . \square

For the rest of the section, the term ‘‘equi- M set’’ will be referring to the equi-Mandelbrot set of the network, which is the intersection of the three node-specific sets. We illustrate the equi- M set for the three models and for different levels of cross talk a , b and f between nodes.

Starting with the simple dual input version of the model, we show in Fig. 3 the effects of changing the level a of talk between the input nodes, on the shape of the equi- M set. It is not surprising that, in both positive and negative a ranges, increasing $|a|$ gradually shrinks the equi-Mandelbrot set. This can be motivated intuitively by the fact that an additional contribution to the node z_2 may cause the critical orbit to increase faster in the z_2 and subsequently the z_3 components; hence, points in the traditional set will no longer be included in the mutants for $a \neq 0$.

As a increases in the positive range, we noticed that the network M sets form nested subsets (which is not true for the negative range), that they remain connected for all values of a , and that the Hausdorff dimension of the boundary increases with a (in Fig. 3, notice an increased wrinkling of the boundary as a takes larger positive values, and an increase smoothing as a takes negative values with increasing absolute value). Perturbations of a in the positive range seem to have a much more substantial contribution to the size of the equi- M set, while perturbations of a in the negative range

have a lesser influence on the size and affect mostly the region close to the boundary of the equi- M set, and the boundary topological details. We will track the same changes in a in the other network models and investigate whether this trend is consistent.

Figure 4 illustrates the evolution of the equi- M set in the case of the model with self-drive, for a grid of positive and negative values of the input connectivity a and of the self-drive b . Below are some simple visual observations based on our numerical computations, to be addressed analytically in future work.

Decreasing b in the negative range produces no alteration of the M sets when $a > 0$. However, it induces dramatic changes in shape and connectivity when $a < 0$. If for $b > 0$ relatively large, increasing a only slightly alters the shape of the set, for small $b > 0$ the size of the set is also altered with increasing a (generating smaller and smaller subsets), and the complexity of its boundary also seems to increase. The effects of varying $a < 0$ for a fixed value of b become more dramatic with decreasing b in the negative range. These effects include changes in shape and topology, the region $a < 0$ and $b < 0$ allowing the M set to break into multiple connected components.

3.2 Uni-Julia sets

In this section, we will track the changes in the uni-Julia set when the parameters of the system change. One of our goals is to test, first in the case of equi-parameters $c \in \mathbb{C}$, then for general parameters in \mathbb{C}^3 , whether a Fatou–Julia-type theorem applies in the case of our three networks.

First, we try to establish a hypothesis for connectedness of uni- J sets, by addressing numerically and visually questions such as: “Is it true that if c is in the equi- M set of a network, then the uni-Julia set is connected?” “Is it true that, if c is not in the equi- M set of the network, then the uni-Julia set is totally disconnected?” Clearly, this is not simply a \mathbb{C}^3 version of the traditional Fatou–Julia theorem, but rather a slightly different result involving the projection of the Julia set onto a uni-slice. Notice that a connected uni- J set in \mathbb{C} may be obtained from a disconnected \mathbb{C}^3 network Julia set and conversely that a disconnected uni- J projection may come from a connected Julia in \mathbb{C}^3 . We will further discuss \mathbb{C}^3 versions of these objects in the context of iterations of real variables, where one can visualize

the full Mandelbrot and Julia sets for the network as subsets of \mathbb{R}^3 . Here, we will first investigate uni- J sets for equi-parameters $(c_1, c_2, c_3) = (c, c, c)$, with a particular focus on tracking the topological changes in the uni- J set as the system approaches the boundary of the equi- M set and leaves the equi- M set.

First, we fix the network type and the connectivity profile (i.e., the parameters a, b and f), and we observe how the uni- J sets evolves as the equi-parameter c changes. In Figs. 5 and 6, we illustrate this for two examples of self-driven models: one with $b = -1$ and $a = 0$, the other with $b = -1/3$ and $a = -2/3$. As the parameter point (c, c, c) approaches the boundary of the equi- M set, the topology of the uni- J set is affected, with its connectivity breaking down “close to” the boundary.

Second, we look at the dependence of uni-Julia sets on the coupling profile (network type). As an example, we fixed the equi-parameter $c = -0.117 - 0.76i$, and we first considered a simple dual network with negative feed-forward and small cross talk $a = -0.05$. We then added self-drive $b = -1$ to the output node and then additionally introduced negative feedback $f = -0.75$. The three resulting uni-Julia sets are shown in Fig. 7. Notice that a small degree of feedback f produces a more substantial difference than a larger change in the self-drive b .

Third, one can study the dependence of uni-Julia sets on the strength of specific connections within the network. As a simple illustration of how complex this dependence may be, we show in Figs. 8 and 9 the effects on the uni- J sets of slight increases in the cross talk parameter a , for two different values of the equi-parameter c .

An immediate observation is that for uni- J sets, the dichotomy from traditional single-map iterations no longer stands: uni- J sets can be connected, totally disconnected, but can also be disconnected into a (finite or infinite) number of connected components, without being totally disconnected. Based on our illustrations, we can further conjecture, in the context of our three models, a description of connectedness for uni- J sets, as follows:

Conjecture 3.4 *For any of the three models described, and for any equi-parameter $c \in \mathbb{C}$, the uni- J set is connected only if c is in the equi- M set of the network, and it is totally disconnected only if c is not in the equi- M set of the network.*

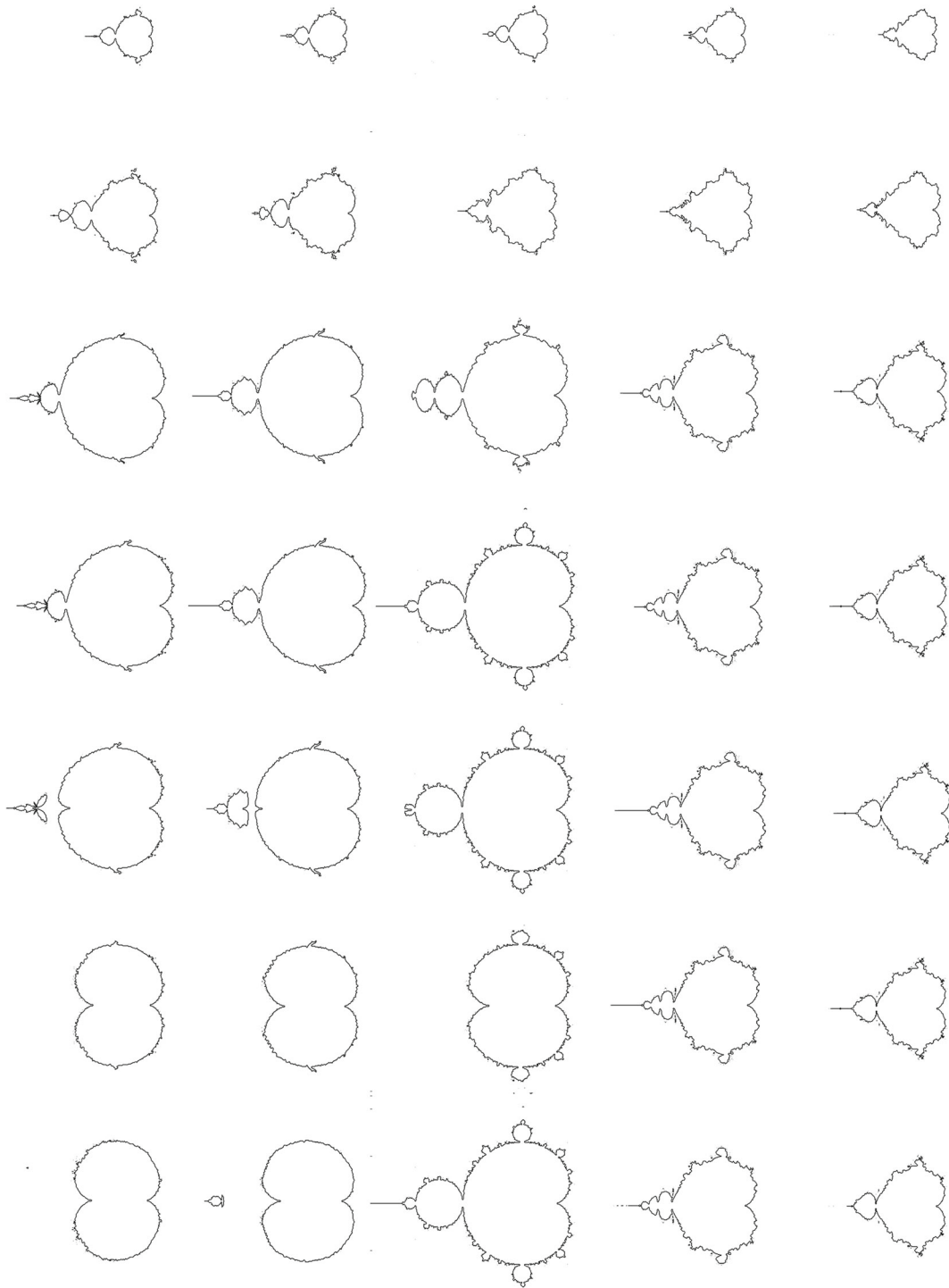


Fig. 4 Equi- M sets for the model variation 2 (with self-drive), for different values of the parameters a and b . The rows show, from bottom to top, increasing values of the self-drive: $b = -1$, $b = -2/3$; $b = -1/3$; $b = 0$ (this row representing the simple dual model, as shown in Fig. 3); $b = 1/3$; $b = 2/3$; $b = 1$. The

columns show, from left to right, increasing values of cross talk between the two input nodes: $a = -2/3$, $a = -1/3$, $a = 0$, $a = 1/3$ and $a = 2/3$. All the equi- M sets were generated from $L = 100$ iterations and plotted at the same scale, in the complex square $[-1.75, 1.25] \times [-1.5, 1.5]$

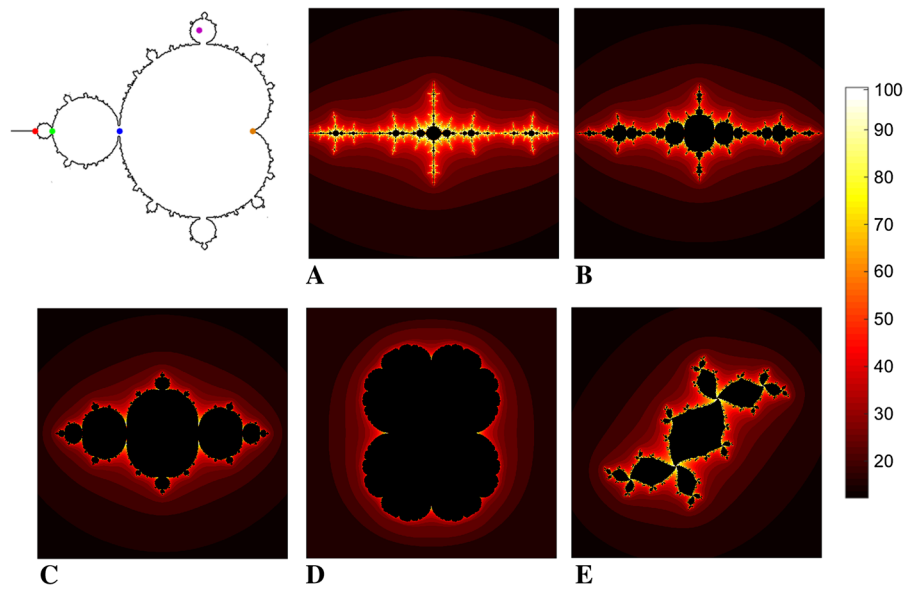


Fig. 5 Uni-Julia sets for a self-drive network with $a = 0$ and $b = -1$, for different values of the equi-parameter c (marked with colored dots on the equi- M template in upper left): **a** $c = -1.38$ (red), **b** $c = -1.25$ (green), **c** $c = -0.75$ (blue), **d** $c = 0.25$ (orange) and **e** $c = -0.15 + 0.75i$ (purple). Both equi- M and uni- J sets coincide in this case with the traditional Mandelbrot and Julia sets for single-map iterations. All sets were based on

100 iterations. The *color map* (also shown along the *color bar* on the right) represents, on a scale from 1 (darkest) to 100 (lightest), the number of iterations necessary for each point in the \mathbb{C} plane to escape the disk of radius 2 around the origin. The filled uni-Julia sets, of points which never escape, are shown in black. (Color figure online)

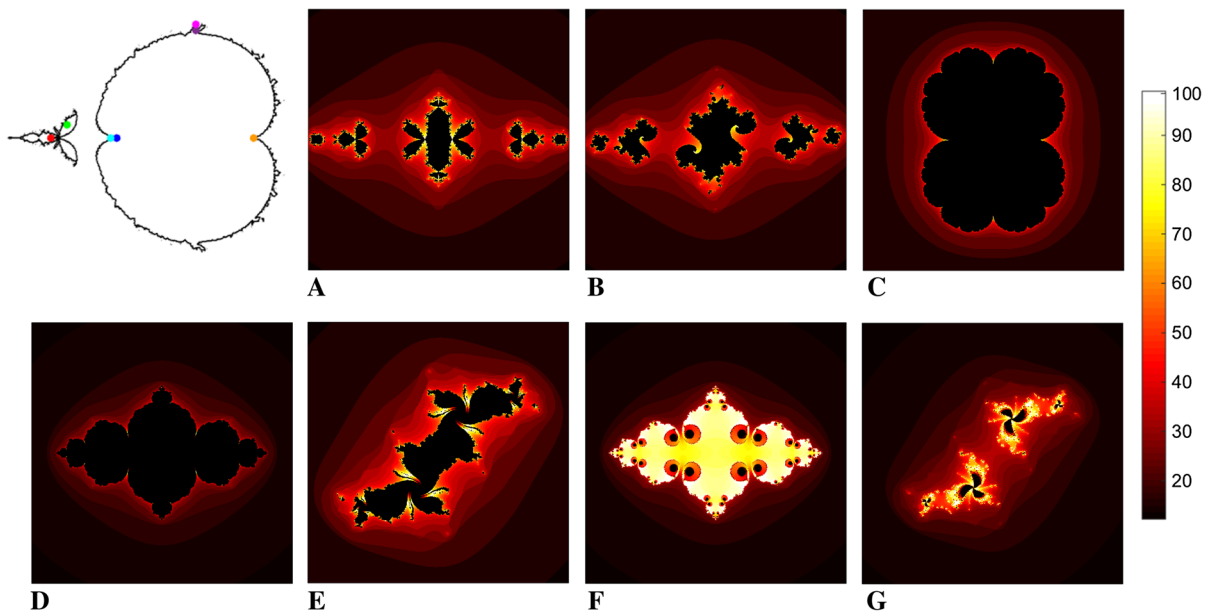


Fig. 6 Uni-Julia sets for a self-drive network with $a = -2/3$ and $b = -1/3$, for different values of the equi-parameter c (marked with colored dots on the equi- M template in upper left): **a** $c = -1$ (red), **b** $c = -0.9 + 0.08i$ (green), **c** $c = 0.25$ (orange), **d** $c = -0.595$ (blue), **e** $c = -0.11 + 0.66i$ (dark purple), **f** $c = -0.63$ (cyan), **g** $c = -0.11 + 0.7i$ (magenta). For the first four panels, c is in the equi- M set; for the last two, c is outside of

the equi- M set. All sets were based on 100 iterations. The *color map* (also shown along the *color bar* on the right) represents, on a scale from 1 (darkest) to 100 (lightest), the number of iterations necessary for each point in the \mathbb{C} plane to escape the disk of radius 2 around the origin. The filled uni-Julia sets, of points which never escape, are shown in black. (Color figure online)

Fig. 7 Evolution of the uni-Julia set for fixed equi-parameter $c = -0.117 - 0.76i$, as the network profile is changed, from **a** simple dual with $a = -0.05$, to **b** self-drive with additional $b = -1$, to **c** feedback with additional $f = -0.75$

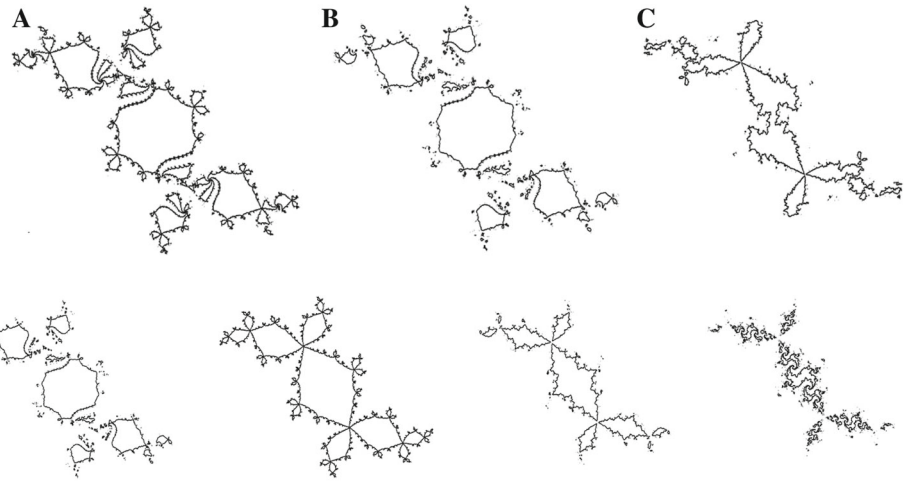


Fig. 8 Evolution of the uni-Julia set for a self-drive network with $b = -1$ and equi-parameter $c = -0.117 - 0.76i$, as the input cross talk a is increased. The panels show, left to right: $a = -0.07$, $a = -0.05$, $a = 0$, $a = 0.05$ and $a = 0.07$

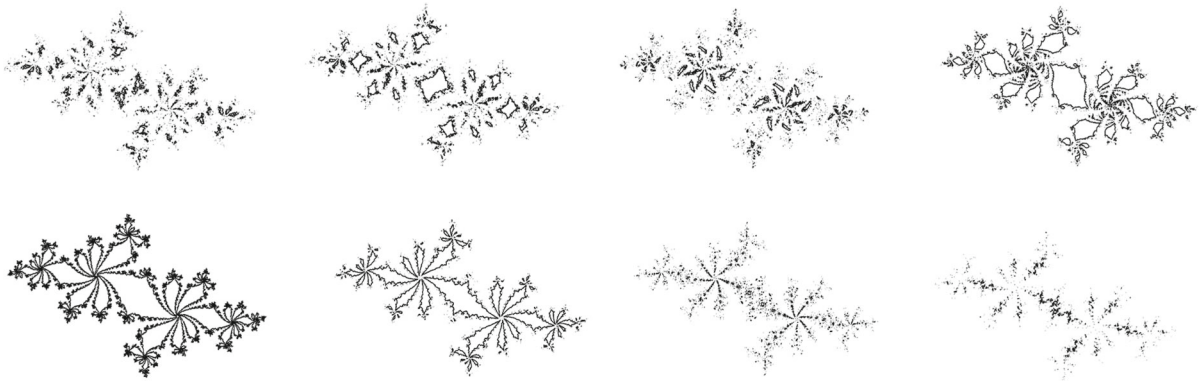


Fig. 9 Evolution of the uni-Julia set for a self-drive network with $b = -1$ and equi-parameter $c = -0.62 - 0.432i$, as the input cross talk a is increased. The panels show, in order: $a = -0.022$,

$a = -0.02$, $a = -0.015$, $a = -0.01$, $a = 0$, $a = 0.01$ and $a = 0.015$, $a = 0.02$

Remark The conjecture implies a looser dichotomy regarding connectivity of uni- J sets than that delivered by the traditional Fatou–Julia result for single maps: If c is in the equi- M set of the network, then the uni- J set is either connected or disconnected, without being totally disconnected. If c is not in the equi- M set of the network, then the uni- J set is disconnected (allowing in particular the case of totally disconnected). Finally, we want to remind the reader that uni-Julia sets can be defined for general parameters $(c_1, c_2, c_3) \in \mathbb{C}^3$, as shown in Fig. 10.

4 Real case

The same definitions apply for iterations of real quadratic maps, with the real case presenting the advantage of easy visualization of full Julia and Mandelbrot sets, rather than having to consider equi-slices, as we did in the complex case. In Figs. 11 and 12, we illustrate a few multi- M and multi- J sets, respectively, for some of the same networks considered in our complex case.

Fig. 10 Uni-Julia sets for a general parameter $(c_1, c_2, c_3) \in \mathbb{C}^3$, with $c_1 = -0.75$, $c_2 = -0.117 - 0.76i$ and $c_3 = -0.62 - 0.432i$. The panels represent uni- J sets for a self-drive network with $b = -1$, as the cross talk a changes from **a** $a = 0$, to **b** $a = 0.1$, to **c** $a = 0.15$

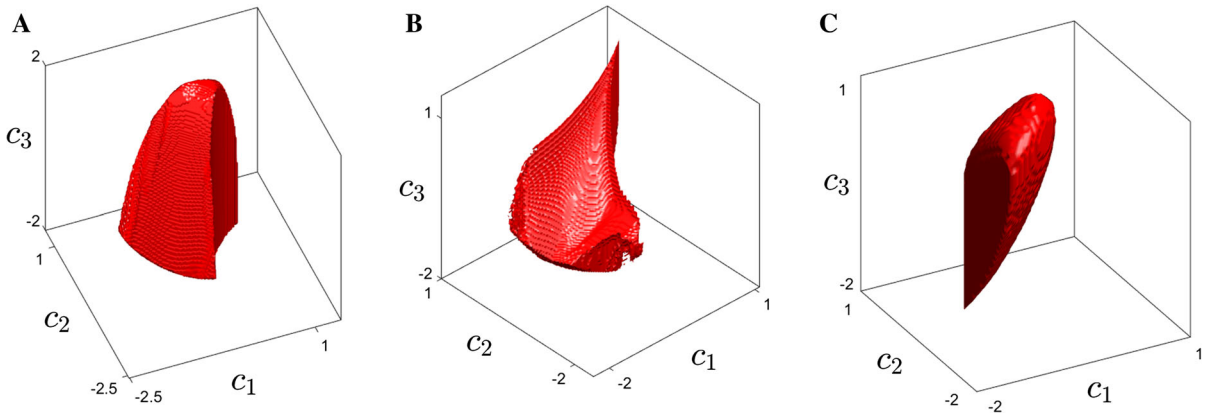
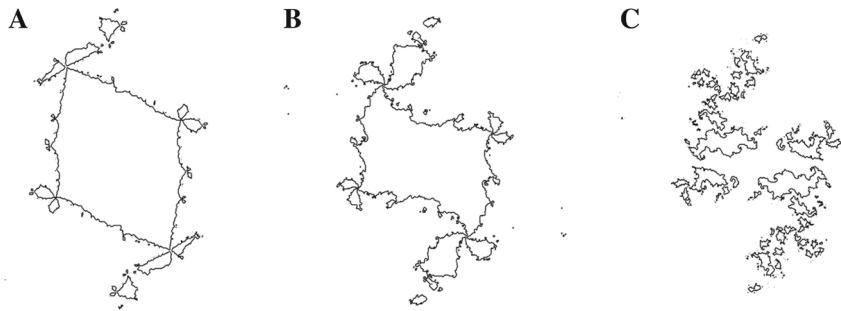


Fig. 11 Real network Mandelbrot sets in the parameter space $(c_1, c_2, c_3) \in \mathbb{R}^3$. **a** Simple dual network with $a = -1$. **b** Self-drive network with $a = -1$ and $b = 1$. **c** Self-drive network with

$a = 1/2$ and $b = 1$. Plots were generated with 50 iterations and in resolution 200^3

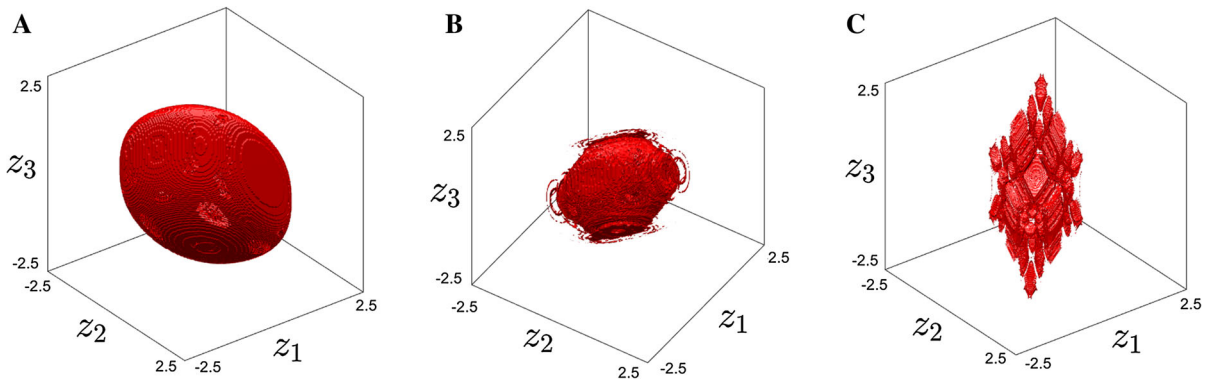


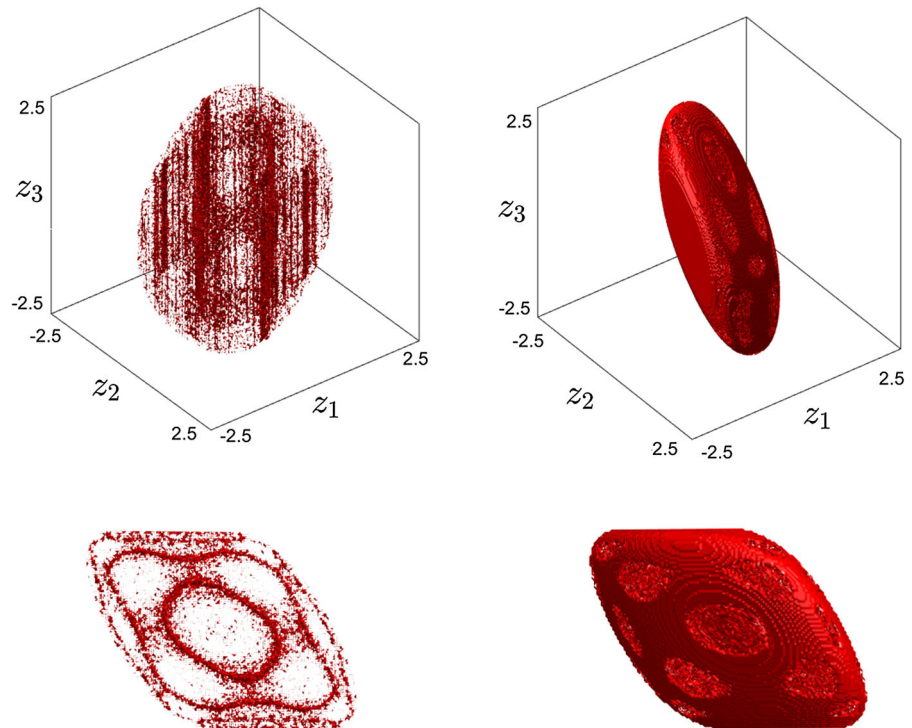
Fig. 12 Real network Julia sets in the node-variable space $(z_1, z_2, z_3) \in \mathbb{R}^3$. The first two panels represent self-drive networks with $a = 1/2$ and $b = 1$, with equi-parameters, respectively: **a** $c = -0.589$, **b** $c = -0.4 - 0.08i$. **c** The third panel

shows the self-drive network with $a = 0$ and $b = -1$, for $c = -0.62 - 0.432i$. Plots were generated with 50 iterations and in resolution 200^3

Moving to illustrate the *relationship* between the multi- M and the multi- J set in this case, consider, for example, the self-drive real network with $a = 1/2$ and $b = 1$, for different multi-parameters (c_1, c_2, c_3) . While more computationally intensive, higher-

resolution figures would be necessary to establish the geometry and fractality of these sets, one may already notice basic properties. For example, Fig. 12 shows that if one were to consider complex equi-parameters, the multi-Julia set may not only be connected (Fig. 12a), or

Fig. 13 Real network Julia sets for the self-drive model with $a = 1/2$ and $b = 1$. The two multi-parameters $(c_1, c_2, c_3) = (-0.5, -0.7, -0.7)$ (left panels) and $(c_1, c_2, c_3) = (-0.5, -0.7, -0.6)$ (right panels) are not in the Mandelbrot set for the network. The top row shows the 3-dimensional Julia sets, and the bottom panels show top views of the same sets. Plots were generated with 50 iterations and in resolution 200^3



totally disconnected (not shown), but may also be broken into a number of connected components (Fig. 12b, c).

This remained true when imposing the restriction for our multi-parameters to be in \mathbb{R}^3 , once we allow arbitrary (that is, not necessarily equi) parameters. The panels of Fig. 13 show the multi- J sets for two different, but close parameters, $(c_1, c_2, c_3) = (-0.5, -0.7, -0.7)$ and $(c_1, c_2, c_3) = (-0.5, -0.7, -0.6)$, respectively, both of which are not in the multi- M set. The figures suggest a disconnected (although not totally disconnected) multi- J set in the first case and a connected multi- J set in the second case. This implies that the traditional Fatou–Julia dichotomy fails in this context—and that the statement relating boundedness of the critical orbit with connectedness of the multi- J set does not hold for real networks. More precisely, we found parameters for which the multi-Julia set appears to be connected, although the critical multi-orbit is unbounded. On the other hand, the counterpart of the theorem may still hold, in the following form: “If the parameter belongs to the multi- M set, then the multi- J set is connected.”

Part of our current visual investigations consists in running optimized numerical algorithms computing multi- M and multi- J sets in \mathbb{R}^3 , with high enough

resolution to allow (1) observation of possible fractal properties of multi- J and of multi- M set boundaries and (2) computation of the genus of the filled multi- J sets, in attempt to phrase a topological extension of the theorem that takes into account the number of handles and tunnels that open up in these sets as their connectivity breaks down when leaving the Mandelbrot set.

5 Discussion

5.1 Comments on our results

In this paper, we used a combination of analytical and numerical approaches to propose possible extensions of Fatou–Julia theory to networked complex maps. Broadly, our paper suggests a new direction of study, with potentially tractable, although complex mathematical questions. While existing results do not apply in their traditional form to the context of networks, it appears that connectivity of uni-Julia and multi-Julia sets may still be strongly influenced by the behavior of the critical orbit. We conjectured weaker extensions of the Fatou–Julia theorem, based thus far only on numerical inspection, and which remain subject to a rigorous study that would support or refute them.

Our line of study includes understanding and interpreting the importance of this type of results in the context of networks from natural sciences. One potential view, proposed by the authors in their previous joint work, is to interpret iterated orbits as describing the temporal evolution of an evolving system (e.g., copying and proofreading DNA sequences, or learning in a neural network). Along these lines, an initial condition which escapes to ∞ under iterations may represent a feature of the system which becomes in time unsustainable, while an initial condition which is attracted to a simple periodic orbit may represent a feature which is too simple to be relevant or efficient for the system. Then, the points on the boundary between these two behaviors (i.e., the Julia set) may be viewed as the set of optimal features, allowing the system to operate in a dynamic regime ideal for performing its complex function. One can try to interpret the current results in light of how this “optimal set of features” changes when perturbing the network’s architecture.

Philosophically, one may interpret that in the case of a network with connected Julia set, all sustainable initial conditions (i.e., initial points leading to bounded orbits) can be reached by perturbations from rest (i.e., from the critical point, with all nodes set at zero), without having to leave the filled Julia set to get from one initial condition to the other. At the other end of the spectrum, totally disconnected Julia sets may characterize pathological networks with only a dust of scattered initial states leading to sustainable dynamics. Unlike in the traditional Fatou–Julia theory, networks allow for the intermediate case of Julia sets which are disconnected, without being totally disconnected. Multiple connected components for the Julia set may correspond conceptually to different healthy functional ranges that are accessible to a network/individual and may be the mark of a healthy system, capable to respond more swiftly to changes in the initial state by tuning to different—yet still sustainable—asymptotic dynamics.

Along the same lines, we defined the Mandelbrot set as the structural node range (range of node-wise dynamic parameters c) for which the network is functionally sustainable when started at rest (the orbit does not escape when all nodes are initiated at zero). One of our aims was to question whether this range coincides with the parameter locus for which the Julia set is connected. The answer was “no” in the case of networks with real nodes, as well as in the context of complex slices for identical node maps (equi-parameters c) and

identical node-wise initial conditions (uni-Julia sets). However, a weaker statement seems to hold, in the sense that one always has to traverse an intermediate asymptotic region characterized by disconnected Julia sets when transitioning from a parameter regime of connected Julia sets (always inside the Mandelbrot set) to a regime of totally disconnected Julia sets (always outside of the Mandelbrot set).

One of our first observations was that even in networks where all nodes are identical maps, their behavior may not be “synchronized,” in the sense that different nodes may have different asymptotic behavior (reflected in topological differences between node-wise Mandelbrot and Julia sets). Node coupling enhances “de-synchronization” between two or more nodes, by differentially shrinking specific node-wise asymptotic sets, the extent of the shrinking being correlated for each node with its afferent connectivity (i.e., node differences being dependent on the network architecture).

We found interesting the idea that additional networking may generally lead to smaller network Mandelbrot and Julia sets than the traditional versions for single decoupled maps. We therefore followed up with a more in-depth investigation on how the topological and fractal behavior of these sets depend on *specific* changes in the network hard wiring. We found instances in which small perturbations in the strength of one single connection may lead to dramatic topological changes in the asymptotic sets, and instances in which these sets are robust to much more significant changes.

For example, our numerical results indicate that introducing feedback in our system has a much more dramatic effect than changing the level of cross talk a between the input nodes (e.g., Figs. 2, 7). This agrees with existing evidence from other discrete dynamic models (e.g., of transcriptional regulatory networks), which found that feed-forward loops provide higher temporal coherence with lower entropy [15]. However, although network data demonstrate the statistical significance between the effects of the two [11, 12], it is not yet clear why feed-forward loops are advantageous over feedback loops in dynamical systems. Understanding analytically the underpinnings of these differences in simple model networks of quadratic maps may shed light on existing numerical and empirical observations in biological networks.

Another interesting observation regards the differences we found between the effects of excitation versus

inhibition in the system. We investigated this question in relation with all our three types of connections (input cross talk, self-drive and feedback strength), by allowing both positive (excitatory) and negative (inhibitory) values for the three corresponding parameters a , b and f , and then comparing the effects. An upturn of excitatory cross talk $a > 0$ generally led to a nesting (and relatively rapid shrinking) of the asymptotic sets (Fig. 3). This is not surprising and supports our intuition that the sustainable network range will shrink if too much feed-forward excitation is added into the system. In the absence of other network influences (that is, for the simple dual model with $b = 0$ and $f = 0$), inhibitory cross talk $a < 0$ led to little changes in the size and topology of the uni- J and equi- M sets and instead affected the Hausdorff dimension of their boundary (perhaps a suggestion that excessive cross talk inhibition may reduce the system's complexity, as reflected in the fractality of its asymptotic sets). Altogether, the main difference between the effects of excitation and inhibition in this case seems to be in the *size* of the sustainable range.

Subsequent simulations (illustrated in the following figures) clarified that, as one would expect, the self-drive b and the feedback f gate and modulate the effect of the input cross talk. For example, when introducing an additional small $b < 0$, increasing the inhibitory cross talk $a < 0$ did not consistently affect the size of the uni- J set more than a comparable increase in excitatory cross talk $a > 0$. However, even slight levels of inhibition were able to break down the uni- J set into connected components, more effectively than by introducing much higher levels of excitation (Figs. 8, 9). This ability of inhibition to affect connectivity remained true for the equi- M sets (Fig. 4, with the sets beginning to break into disconnected components in the bottom left panels, for $a < 0$). On the other hand, we noticed that a positive self-drive $b > 0$ canceled both size and connectivity effects subsequent to boosting cross talk in the simple dual model. Indeed, for $b = 1$ (Fig. 4, top row), the equi- M sets for all a , positive *or* negative, look very similar. A complex network (the brain in particular) may have to know in advance, and be able to do so, which hardwired structure is most effective to use in order to obtain either or both effects, and how to plastically modify this structure on a continuous basis, adapting online to new behavioral requirements and restrictions.

5.2 Future work

There are a few interesting aspects which we aim to address in our future work on iterated networks. For example, we are interested in studying the structure of equi- M and uni- J sets for larger networks, and in understanding the connection between the network architecture and its asymptotic dynamics. This direction can lead to ties and applications to understanding functional networks that appear in the natural sciences, which are typically large.

The authors' previous work has addressed some of these aspects in the context of continuous dynamics and coupled differential equations. However, when translating network architectural patterns into network dynamics, the great difficulty arises from a combination of the graph complexity and the system's intractable dynamic richness. Addressing the question at the level of low-dimensional networks can help us more easily identify and pair specific structural patterns to their effects on dynamics and thus better understand this dependence. The next natural step is to return to the search for a similar classification in high-dimensional networks, where specific graph measures or patterns (e.g., node degree distribution, graph Laplacian, presence of strong components, cycles or motifs) may help us, independently or in combination, classify the network's dynamic behavior.

Of high interest are methods that can identify robust versus vulnerable features of the graph from a dynamic standpoint. As Figs. 14 and 15 show, it is clear that a small perturbation of the graph (e.g., adding a single edge) has the potential, even for higher-dimensional networks, to produce dramatic changes in the asymptotic dynamics of the network and readily leads to substantially different M and J sets. However, this is not consistently true. We would like to understand whether a network may have a priori knowledge of which structural changes are likely to produce large dynamic effects. This is a real possibility in large natural learning networks, including the brain—where such knowledge probably affects decisions of synaptic restructuring and temporal evolution of the connectivity profile.

Once we gain enough knowledge of networked maps for fixed nodes and edges, and we formulate which applications this framework may be appropriate to address symbolically, we will allow the nodes' dynamics, as well as the edge weights and distribution, to evolve in time together with the iterations. This

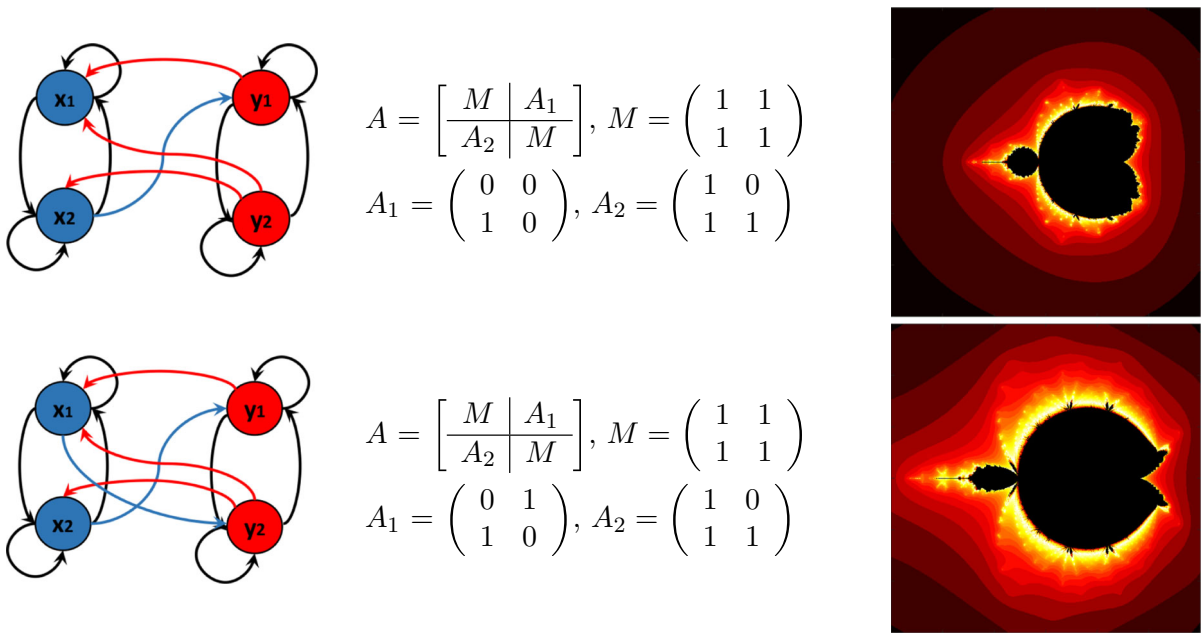


Fig. 14 Equi- M sets for two bipartite networks of size $N = 4$ described schematically on the left, together with their adjacency matrices. Both systems have connectivity parameters

$g_{xx} = g_{yy} = 1/2$ (between *same-color* nodes), $g_{xy} = g_{yx} = -1/2$ (between nodes of *different colors*). (Color figure online)

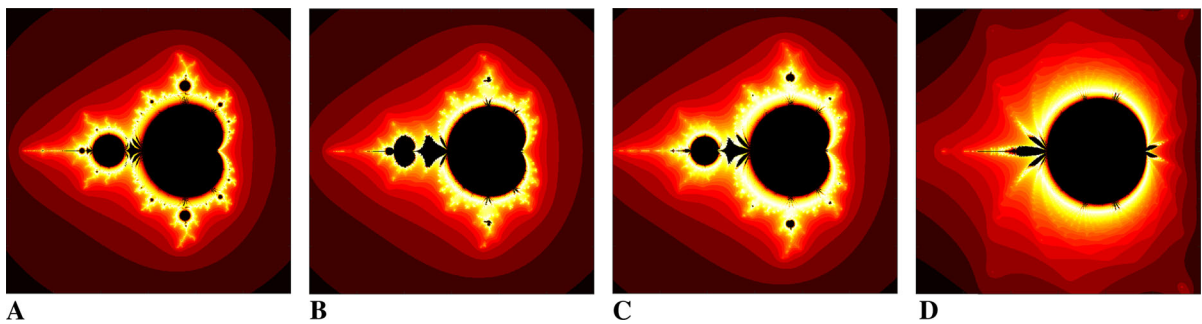


Fig. 15 Equi- M sets for a bipartite network with 20 nodes, formed of two cliques X and Y , with $N = 10$ nodes in each. The adjacency matrix is therefore similar to those in Fig. 14, with *square blocks* M , A_1 and A_2 of size $N = 10$. The densities (number of ones in each block, i.e., number of X -to- Y and, respectively, Y -to- X connecting edges) were taken in *each panel*

to be (out of the total of $N^2 = 100$): **a** $N_{xy} = N_{yx} = 10$, **b** $N_{xy} = 15, N_{yx} = 10$, **c** $N_{xy} = N_{yx} = 15$, **d** $N_{xy} = N_{yx} = 50$. In all cases, the connectivity parameters (i.e., edge weights) were $g_{xx} = g_{yy} = 1/10$ (between nodes within the *same clique* X or Y) and $g_{xy} = g_{yx} = -1/10$ (between nodes in *different cliques*). (Color figure online)

process may account for phenomena such as learning or adaptation—a crucial aspect that needs to be understood about systems. This represents a natural direction in which to extend existing work by the authors on random iterations in the one-dimensional case.

Acknowledgments The work on this project was supported by the SUNY New Paltz Research Scholarship and Creative Activities program, and by the SUNY New Paltz Provost Challenge Grant. We additionally want to thank Sergio Verduzco-Flores, for his programming suggestions, and Mark Comerford, for the useful mathematical discussions.

Appendix: Uni- J sets for higher-dimensional networks

The figures show four uni- J sets, for $N = 4$ and $N = 8$ nodes. The equi-parameters, adjacency matrices and connectivity parameters of each network are given in Figs. 16, 17, 18 and 19.

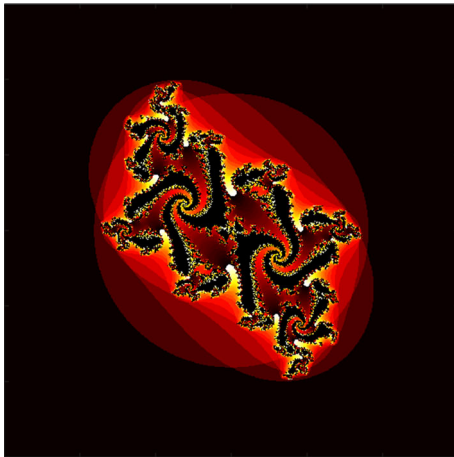


Fig. 16 Size $N = 4$, equi-parameter $c = -0.117 - 0.76i$. Adjacency: $A = \begin{bmatrix} M & A_1 \\ A_2 & M \end{bmatrix}$, where $M = \begin{pmatrix} 1 & 1 \\ 1 & 1 \end{pmatrix}$, $A_1 = \begin{pmatrix} 1 & 0 \\ 0 & 0 \end{pmatrix}$, $A_2 = \begin{pmatrix} 1 & 0 \\ 1 & 0 \end{pmatrix}$. Connectivity parameters: $g_{xx} = g_{yy} = 1/2$, $g_{xy} = g_{yx} = -1/2$

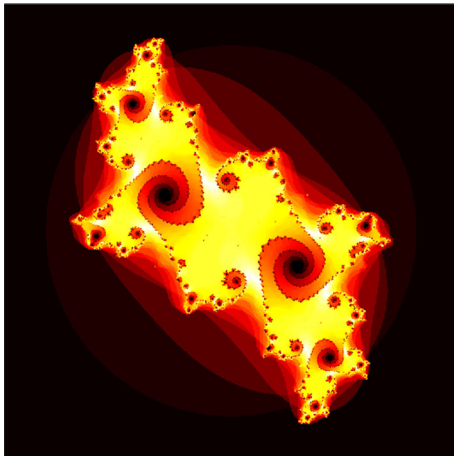


Fig. 17 Size $N = 4$, equi-parameter $c = -0.117 - 0.856i$. $A = \begin{bmatrix} M & A_1 \\ A_2 & M \end{bmatrix}$, where $M = \begin{pmatrix} 1 & 1 \\ 1 & 1 \end{pmatrix}$, $A_1 = \begin{pmatrix} 0 & 1 \\ 0 & 0 \end{pmatrix}$, $A_2 = \begin{pmatrix} 1 & 0 \\ 1 & 1 \end{pmatrix}$. Connectivity parameters: $g_{xx} = g_{yy} = 1/2$, $g_{xy} = g_{yx} = -1/2$

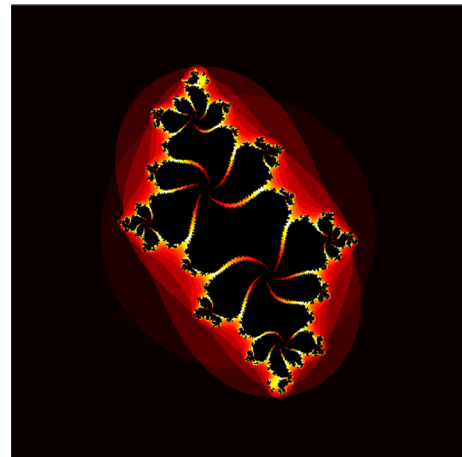


Fig. 18 Size $N = 4$, equi-parameter $c = -0.5622 - 0.62i$. $A = \begin{bmatrix} M & A_1 \\ A_2 & M \end{bmatrix}$, where $M = \begin{pmatrix} 1 & 1 \\ 1 & 1 \end{pmatrix}$, $A_1 = \begin{pmatrix} 0 & 1 \\ 0 & 0 \end{pmatrix}$, $A_2 = \begin{pmatrix} 1 & 0 \\ 1 & 0 \end{pmatrix}$. Connectivity parameters: $g_{xx} = g_{yy} = 1/2$, $g_{xy} = g_{yx} = -1/2$

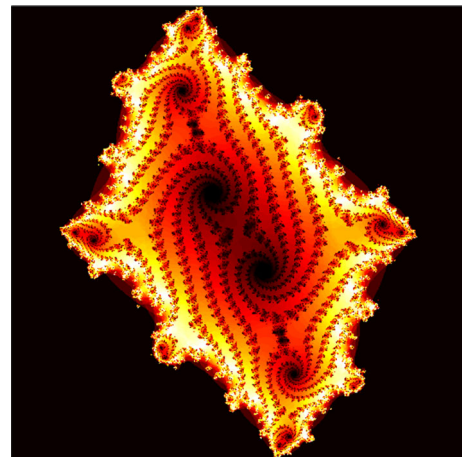


Fig. 19 Size $N = 8$, equi-parameter $c = -0.62 - 0.62i$. $A = \begin{bmatrix} M & A_1 \\ A_2 & M \end{bmatrix}$, where $M = \begin{pmatrix} 1 & 1 & 1 & 1 \\ 1 & 1 & 1 & 1 \\ 1 & 1 & 1 & 1 \\ 1 & 1 & 1 & 1 \end{pmatrix}$, $A_1 = \begin{pmatrix} 1 & 0 & 1 & 1 \\ 1 & 1 & 1 & 0 \\ 1 & 0 & 0 & 0 \\ 0 & 1 & 0 & 0 \end{pmatrix}$, $A_2 = \begin{pmatrix} 0 & 0 & 0 & 0 \\ 0 & 1 & 1 & 1 \\ 1 & 1 & 0 & 1 \\ 0 & 1 & 1 & 0 \end{pmatrix}$. Connectivity parameters: $g_{xx} = g_{yy} = 1/4$, $g_{xy} = g_{yx} = -1/4$

References

1. Atay, F.M., Jost, J., Wende, A.: Delays, connection topology, and synchronization of coupled chaotic maps. *Phys. Rev. Lett.* **92**(14), 144101 (2004)

2. Branner, B., Hubbard, J.H.: The iteration of cubic polynomials part II: patterns and parapatterns. *Acta Math.* **169**(1), 229–325 (1992)
3. Brunel, N.: Dynamics of sparsely connected networks of excitatory and inhibitory spiking neurons. *J. Comput. Neurosci.* **8**(3), 183–208 (2000)
4. Bullmore, E., Sporns, O.: Complex brain networks: graph theoretical analysis of structural and functional systems. *Nat. Rev. Neurosci.* **10**(3), 186–198 (2009)
5. Carleson, L., Gamelin, T.W.: *Complex Dynamics*, vol. 69. Springer Science & Business Media, New York (1993)
6. Devaney, R.L., Look, D.M.: A criterion for Sierpinski curve Julia sets. In: *Topology Proceedings*, vol. 30, pp. 163–179 (2006)
7. Fatou, P.: Sur les équations fonctionnelles. *Bull. Soc. Math. Fr.* **47**, 161–271 (1919)
8. Gray, R.T., Robinson, P.A.: Stability and structural constraints of random brain networks with excitatory and inhibitory neural populations. *J. Comput. Neurosci.* **27**(1), 81–101 (2009)
9. Isaeva, O.B., Kuznetsov, S.P., Osbaldestin, A.H.: Phenomena of complex analytic dynamics in the systems of alternately excited coupled non-autonomous oscillators and self-sustained oscillators. *arXiv preprint arXiv:1011.4175* (2010)
10. Julia, G.: Mémoire sur l'itération des fonctions rationnelles. *J. Math. Pures Appl.* **1**, 47–246 (1918)
11. Kee, T., Sanda, P., Gupta, N., Stopfer, M., Bazhenov, M.: Feed-forward versus feedback inhibition in a basic olfactory circuit. *PLoS Comput. Biol.* **11**(10), e1004531 (2015)
12. Klemm, K., Bornholdt, S.: Topology of biological networks and reliability of information processing. *Proc. Natl. Acad. Sci. USA* **102**(51), 18414–18419 (2005)
13. Marcus, C.M., Westervelt, R.M.: Dynamics of iterated-map neural networks. *Phys. Rev. A* **40**(1), 501 (1989)
14. Masoller, C., Atay, F.M.: Complex transitions to synchronization in delay-coupled networks of logistic maps. *Eur. Phys. J. D* **62**(1), 119–126 (2011)
15. Oosawa, C., Takemoto, K., Savageau, M.A.: Effects of feedback and feedforward loops on dynamics of transcriptional regulatory model networks. *ArXiv preprint arXiv:0711.2730* (2007)
16. Rădulescu, A., Verduzco-Flores, S.: Nonlinear network dynamics under perturbations of the underlying graph. *Chaos: an Interdisciplinary J. Nonlinear Sci.* **25**(1), 013116 (2015)
17. Rădulescu, A., Pignatelli, A.: Symbolic template iterations of complex quadratic maps. *Nonlinear Dyn.* **84**(4), 2025–2042 (2016)
18. Siri, B., Quoy, M., Delord, B., Cessac, B., Berry, H.: Effects of hebbian learning on the dynamics and structure of random networks with inhibitory and excitatory neurons. *J. Physiol. Paris* **101**(1), 136–148 (2007)
19. Sporns, O.: Graph theory methods for the analysis of neural connectivity patterns. In: *Neuroscience Databases: A Practical Guide*, pp. 171–186. Springer (2003)
20. Sporns, O.: The non-random brain: efficiency, economy, and complex dynamics. *Front. Comput. Neurosci.* **5**, 5 (2011)
21. Wang, Xin: Period-doublings to chaos in a simple neural network: an analytical proof. *Complex Syst.* **5**(4), 425–444 (1991)
22. Yu, X., Jia, Z., Jian, X.: Logistic mapping-based complex network modeling. *Appl. Math.* **4**(11), 1558 (2013)